scientific reports

Check for updates

OPEN

# Resveratrol improved mitochondrial biogenesis by activating SIRT1/PGC-1α signal pathway in SAP

Shu-kun Wu[1,2,3], Le Wang[1,3], Fang Wang[1]✉ & Jiong Zhang[1]✉

**NLRP3 inflammasomes- pyroptosis axis is activated by microcirculation dysfunction and touched off severe acute pancreatitis (SAP). Activation of PGC-1α can improve microcirculation dysfunction by promoting mitochondrial biogenesis. Resveratrol (RSV), one typical SIRT1 agonist, possesses the ability of alleviating SAP and activing PGC-1α. Therefore, the study was designated to explore whether the protective effect of RSV in SAP was though suppressing NLRP3 inflammasomes- pyroptosis axis via advancing SIRT1/PGC-1α-dependent mitochondrial biogenesis. The models of SAP were induced by treating with sodium taurodeoxycholate in rats and AR42J cells. The pathological injury, water content (dry/wet ratio) and microcirculation function of pancreas, activity of lipase and amylase were used to evaluate pancreatic damage. The expression of inflammatory cytokine was measured by ELISA and RT-PCR. The damage of mitochondrial was evaluated by measuring the changes in Mitochondrial Membrane Potential (ΔΨm), mitochondrial ROS, ATP content and MDA as well as relocation of mtDNA and the activity of SOD and GSH. The expressions of NLRP3 inflammasomes- pyroptosis axis proteins were detected by Western blotting as well as SIRT1/PGC-1α/NRF1/TFAM pathway protein. Moreover, the modification of PGC-1α was measured by co-immunoprecipitation. The results displayed that RSV can significantly improve the damage of pancreas and mitochondrial, decrease the expression of pro-inflammatory factor and the activation of NLRP3 inflammasomes- pyroptosis axis, promote the expression of an-inflammatory factor and the deacetylation of PGC-1α together with facilitating SIRT1/PGC-1α-mediating mitochondrial biogenesis. Therefore, the protective effect of RSV in SAP is though inactivation of NLRP3 inflammasomes- pyroptosis axis via promoting mitochondrial biogenesis in a SIRT1/PGC-1α-dependent manner.**

**Keywords** Resveratrol, Severe acute pancreatitis, Mitochondrial biogenesis, NLRP3 inflammasomes-pyroptosis axis, SIRT1/PGC-1α

Acute pancreatitis (AP) is a common disease in clinical practice[1,2]. Although most AP patients have mild cases, which often self-resolve, approximately 20% develop moderate to severe acute pancreatitis (SAP), accompanied by pancreatic tissue necrosis and organ failure, with a mortality rate of up to 20–40%[3,4]. Despite major progress in SAP diagnosis and treatment modalities in recent decades, the mortality of SAP remains high owing to the paucity of highly effective treatments[3,4]. Therefore, further studies are needed to understand the pathogenesis of SAP and to identify novel diagnostic and treatment tools for this disease to improve patient outcomes.

Current research suggests that the development of SAP is closely associated with $Ca^{2+}$ dysfunction in pancreatic acinar cells, trypsinogen activation, mitochondrial dysfunction, impaired autophagy, endoplasmic reticulum stress, etc[3–5]. Notably, recent studies have confirmed that pyroptosis, a novel form of programmed cell death, plays a crucial role in the development and progression of SAP[6]. Inhibiting pyroptosis in pancreatic acinar cells (which develops from the activation of caspase family proteins via the cleavage of GSDMD) can significantly alleviate pancreatic injury and improve SAP by suppressing the release of inflammatory factors in cells and relieving systemic inflammation[6]. Moreover, caspase family-mediated pyroptosis is achieved via the activation of NLRP3 inflammasomes[6,7]; deactivation of these inflammasomes can inhibit the pyroptosis of pancreatic acinar

[1]Division of Nephrology, Sichuan Provincial People's Hospital & Sichuan Academy of Sciences, University of Electronic Science and Technology, Chengdu, China. [2]Division of Nephrology, Tongji Hospital, Tongji Medical College, Huazhong University of Science and Technology, Wuhan, China. [3]These authors contributed equally: Shu-kun Wu and Le Wang. ✉email: wqqf1121@sina.com; zhangjiong831224@163.com

cells in SAP[6,7]. Therefore, suppressing the NLRP3 inflammasome-pyroptosis axis is a promising technique for alleviating SAP.

Mitochondria are critical cellular organelles with various functions, including energy conversion, oxidative phosphorylation, and calcium storage[8]. Among the aforementioned functions, the role of mitochondria in providing energy for various cellular activities via energy conversion is particularly significant[8]. Mitochondrial dysfunction can lead to the activation of the NLRP3 inflammasome-pyroptosis axis by regulating mitochondrial DNA (mtDNA) activity, thus contributing to poor outcomes in septic shock[9]. A recent report confirmed that mitochondrial biogenesis plays an essential role in preserving mitochondrial function and that increasing mitochondrial biogenesis will considerably alleviate mitochondrial dysfunction in AP[10]. Moreover, previous studies have confirmed that mitochondrial biogenesis was promoted by peroxisome proliferator-activated receptor-γ coactivator (PGC)-1α via the regulation of NRF1/TFAM[11,12]. Notably, TFAM can stabilize the levels of mtDNA in the mitochondria and participates in initiating the transcription of mtDNA-encoding genes by binding to mtDNA in the mitochondria[13]. Therefore, targeting PGC-1α may be a promising approach for inhibiting the mtDNA-NLRP3 inflammasome axis in SAP by regulating NRF1/TFAM-mediated mitochondrial biogenesis.

Resveratrol (RSV) is a polyphenolic compound mainly derived from plants, such as peanuts, grapes, and mulberries[14]. It has anti-inflammatory, antioxidant, anti-apoptosis, anti-atherosclerotic, and other pharmacological effects[14]. Molecular pharmacology research has shown that RSV is capable of activating PGC-1α and improving mitochondrial function in AP[15,16]. Considering the influence of RSV on mitochondria, this study aimed to investigate the effect of RSV on NLRP3 inflammasome-mediated pyroptosis in rats with SAP and its relationships with SIRT1, PGC-1α, and mitochondrial biogenesis.

## Materials and methods

### Chemicals and materials

RSV was purchased from Beijing Kaishiyuan Biotechnology Co., Ltd. Enzyme-linked immunosorbent assay (ELISA) kits for amylase and lipase were purchased from Jiancheng Bioengineering Institute (China). Sodium taurocholate (ST) was purchased from Sigma and MCE (USA). The ELISA kits against ET, NO, TXB-2 and 6-K-PGF-1α were obtained from Chongqing Mengbaiou Biotechnology Co., Ltd. JC-1 and ATP assay kits were obtained from Nanjing Jiancheng Bioengineering Institute (Nanjing, China). Antibodies against SIRT1, PGC-1α, NRF1, TFAM, mtDNA, NLRP3, ASC, caspase1, and GSDMD were purchased from Abcam (Cambridge, UK) and ABclonal (Wuhan, China). EX527 (EX), a SIRT1 inhibitor, was obtained from Sigma (USA). SR-18,292, a PGC-1a inhibitor, was obtained from Anjiekai Biological Medicine Technology co., Ltd (Wuhan, China), TargetMol (Boston, MA, USA), and MedchemExpress (New Jersey, USA). A real-time PCR kit was purchased from Toyobo Biolion Technology Co., Ltd (China). PAS staining reagents were obtained from Sichuan Provincial People's Hospital. The PCR primer was purchased from Invitrogen, and the primer sequence is shown in Table 1.

### Animals and treatments

Sixty 6–8-week-old healthy male SD rats (weighing 220–250 g) were purchased from the Experimental Animal Center of Sichuang University and maintained in a standard SPF environment at 60 ± 5% humidity and 25 ± 1 ℃. The animal experimental protocols were approved by the animal care committee of the Sichuan Provincial People's Hospital, and the experimental procedures were conducted in adherence with the NIH Guidelines for the Care and Use of Animals.

The 60 SD rats were randomly divided into four groups ($n = 15$): control (Ctrl), SAP, RSV, and EX527. The rats in all groups were anesthetized with 3% pentobarbital sodium (0.2 mL/100 mg). The SAP model was induced in the SAP, RSV, and EX527 groups via retrograde perfusion of 3.5% ST (1 ml/kg, Sigma, USA) into the biliopancreatic duct[17–19]. The surgical procedures are detailed in the references. The Ctrl group underwent the same procedure, but the ST was not injected. The RSV group was intraperitoneally administered with RSV solution (30 mg/kg) 12 h after administration of ST[18]. The EX527 group was intraperitoneally administered with RSV solution (30 mg/kg) and EX527 (5 mg/kg) 12 h after administration of ST[19]. The Ctrl and SAP groups were treated with the same amount of normal saline. After 72 h, the general status, including postoperative

| Gene | Sense group (5′–3′) | Antisense group (3′–5′) |
|---|---|---|
| TNF-α | GCCACCACGCTCTTCTGTCT | TCTCCCTCCCCAACTCTCCT |
| IL-6 | ATTGTATGAACAGCGATGATGCAC | CCAGGTAGAAACGGAACTCCAGA |
| IL-1β | CCCTGAACTCAACTGTGAAATAGCA | CCCAAGTCAAGGGCTTGGAA |
| IL-18 | ATCAGACCACTTTGGCAGACTTCAC | CTGGGATTCGTTGGCTGTTCGG |
| IL-4 | AGCCCAGGATGCCCTTTAGT | TGATCGTCTTTAGCCTTTCCA |
| IL-10 | AGAAGGACCAGCTGGACAACAT | CAAGTAACCCTTAAAGTCCTG |
| GAPDH | GACATGCCGCCTGGAGAAAC | AGCCCAGGATGCCCTTTAGT |
| ND-1 | TTAATTGCCATGGCCTTCCTCACC | TGGTTAGAGGGCGTATGGGTTCTT |
| β-actin | GGAGATTACTGCCCTGGCTCCTA | GACTCATCGTACTCCTGCTTGCTG |
| SIRT1 | CCCUGUAAAGCUUUCAGAATT | UUCUGAAAGCUUUACAGGGTT |
| PGC-1α | GCACTGACAGATGGAGACGTGA | TCATTGTAGCTGAGCTGAGTGTTGG |

**Table 1**. The primer for RT-PCR.

recovery in food and water consumption, activity, ascites exudation, and wound healing, of all rats was observed. Subsequently, the rats were euthanized via an overdose of 3% pentobarbital sodium, and blood samples and pancreas specimens were collected for further analysis.

### Microcirculation of the pancreas

Each rat was injected with 1.5 mL of FITC-RBC through the tail vein. We measured flow velocity, functional blood vessel number, red blood cell flow, and blood vessel number to evaluate pancreatic microcirculation using the BI-2000 Medical Image Analysis System (Full name: BI-2000 Medical Image Analysis System; Version Number: BI-2000; URL Link: http://www.tme.com.cn/product/70.html, Taimeng Technology Co., Ltd, Chengdu, China). Take pancreatic tissue and homogenize it 3000 r/min, centrifuge at 4 ℃ for 15 min, take the supernatant, then use ELISA assay reagent kits against ET, TXB-2 and 6-K-PGF-1α to measure the content of ET, TXB-2 and 6-K-PGF-1α in rat pancreatic tissue. Nitrate reductase method was used to measure the NO content in pancreatic tissue of rats in each group. Moreover, the ratio of ET/NO and TXB-2/ 6-K-PGF-1α were also calculated.

### Water content assay

The pancreatic water content was evaluated by comparing the dry and wet weights of the pancreas[18]. The pancreas was immediately weighed to obtain the wet weight before being dried in a 48 °C oven for 48 h to obtain the dry weight. The pancreatic wet/dry ratio was calculated based on the following formula: (D/W weight%) = [(dry weight)]/ (wet weight) × 100%.

### Histopathlogy of pancreas

The excised pancreatic tissue was sectioned and mounted in paraffin, after performing Periodic Acid-Schiff (PAS) staining to evaluate the pathological morphology of the pancreas. The pancreas was assayed under a light microscope. Pancreatic tissue was classified by evaluating necrosis + hemorrhage + edema + inflammation according to the modified Kusske scoring standard one the reference[20]. The concrete details are as following. No inflammatory cell infiltration, hemorrhage, edema and necrosis were scored 0; necrosis area (1–10%), hemorrhage and edema (0–25%) were 1 point; necrosis area (11–20%), hemorrhage and edema (25–50%) were 2 points; necrosis area (21–30%), hemorrhage and edema (50–75%) were 3 points; necrosis area (> 30%) hemorrhage and edema (50–55%) were 4 points; 0.5 point for 5 inflammatory cells and 4 points for more than 30 inflammatory cells.

### Cell culture, transfection, interventions, and viability in vitro

The rat pancreatic acinar cell line (AR42J) was purchased from the ATCC (USA). The cells were cultured in Ham's F12K medium containing 200 mL/L fetal bovine serum, 100 kU/L penicillin, and 100 mg/L streptomycin under 5% $CO_2$ and 37 °C conditions. The medium was changed once every 3 days, and the cells were digested with 0.125% trypsin + 0.02% EDTA and subcultured once at 1:3–1:5. For the transfection experiments, AR42J cells were removed and cultured in 6-well plates at a cell density of $10^6$ cells/well for 24 h. The AR42J cell suffered from transfection was cultured with serum-free and antibody free DMEM culture medium at One day before transfection. The SiRNA-SIRT1 or SiRNA-PGC-1α and negative control were designed and synthesized by Genepharma Biotech Co., Ltd in Shang hai. The sequence of SIRT1 and PGC-1α are as shown in Table 1. The concrete steps for cell transfection are following the instructions of LipofectamineTM 2000Reagent (Invitrogen). The LipofectamineTM 2000Reagent were placed in room temperature environment for 5 Min in advance, then mixed it with siRNA-SIRT1/PGC-1α or negative control cells evenly, placed them stand at room temperature for 20 min, then put cell suspension into corresponding cells according to their groups and placed the cells in a cell culture incubator under 5% $CO_2$ and 37 °C conditions. After 6 hours of transfection, the cells were treated with a concentration of 10% serum DMEM medium to further cultivate for 48 h in order to further study. To stimulate AP in vitro, AR42J cells were incubated with 500 μM ST for 3 h as detailed in previous reports[21–23]. As for the control group, the cells were treated with a volume of PBS equivalent to the volume of ST administered for AP induction. To stimulate SIRT1 in vitro, cells were treated with RSV (20μM) for 12 h before AP induction[24]. To suppress PGC-1α in vitro, cells were treated with SR18292 (20 μm) for 12 h before AP induction[25]. Once the intervention time elapsed, 100 μL of CCK-8 solution was added to each well after the medium was collected, and culturing was continued for 2 h in the incubator. The absorbance at 450 nm was measured using an enzyme marker. The collected culture medium was centrifuged to obtain the serum and supernatant.

### Isolation of mitochondria

The mitochondrial isolation kit was purchased from Abcam in UK. The collecting cell and tissue were treated with low-speed centrifugation at 500 ~ 600 g for 5 min to get cell suspension. Then we washed cell suspension for one time with pre-cooled PBS, discarded the supernatant, and added 250 μL buffer A vortex oscillation to resuspended cell fluid in turn. Mitochondria were obtained using a mitochondria isolation kit, according to the manufacturer's instructions.

### Assaying mitochondrial ROS (mROS) and mtDNA levels

Primary pancreatic acinar cells were obtained from rats using a collagenase digestion procedure as described[26]. In brief, fresh pancreas obtained from rats was digested by collagenase IV (200 U/mL) incubation for 19 min at 37 °C. After incubation, pancreas was disintegrated mechanically and filtered through a 100 μm cell strainer and primary acinar cells were obtained by centrifuged at 110 × g for 2 min. The level of mROS in AR42J cells and primary acinar cells were evaluated by use of MitoSox (Invitrogen );The cells were stained with stained with 0.5 μM MitoSOX™ for 30 min at 37 C. Fluorescence intensity was observed with a fluorescence microscope.

The mtDNA was isolated from the pancreas and cell by an mtDNA isolation kit from Abcam in UK. A rat Mitochondrial DNA Copy Number Assay Kit (Xinbosheng, Shenzhen, MCN2) was then used to measure mtDNA copy using qRT-PCR according to the manufacturer's instructions. In brief, the following procedure was used for each 20 μL reaction: 1 μL forward primer, 1 μL reverse primer, 8 μL DNA samples between 0.5 and 3.75 ng/μL, and 10 μL RT-PCR reaction mix. The validated primers to quantify mtDNA and RT-PCR reaction mix were provided by this assay kit.

### Co-immunoprecipitation (Co-IP)

Co-IP was used to evaluate the interactions between PGC-1α proteins and Ace-lys in the nucleus, according to the manufacturer's instructions.

### Measuring amylase, lipase, and inflammatory factor levels

ELISA was used to determine the serum levels of amylase, lipase, IL-8, IL-1β, IL-4, IL-10, TNF-α, and IL-6 in serum.

### Oxidative stress evaluation

Pancreatic tissues were homogenized to obtain the supernatant. Spectrophotometry was applied to determine the activities of superoxide dismutase (SOD) and gluathione (GSH) and the content of malondialdehyde (MDA) in the supernatant by strictly following the instructions of the reagent kit for operation. These reagent kits were obtained from Nanjing Jiancheng Biological Company.

### Detecting activity of SIRT1 deacetylase

SIRT1 deacetylase activity was evaluated using a SIRT1 assay kit (Sigma-Aldrich), according to the manufacturer's instructions. Briefly, proteins were obtained by extraction, and their fluorescence intensities were detected at 340/440 nm.

### Mitochondrial membrane potential (ΔΨ) measurement

Mitochondrial suspension (200 μL) was centrifuged at 5000 rpm for 20 min, and the precipitate was resuspended with 1 mL PBS buffer in a 1.5 mL centrifuge tube. The mixture was then centrifuged again 5000 rpm for 20 min and the supernatant was discarded. Stationary mixture (1.25 mL) was added to the precipitate and incubated at 37 ℃ in the dark for 3 min. Mitochondrial membrane potential (ΔΨ) was evaluated by JC-1 staining according to the manufacturer's instructions (Mitochondrial membrane potential assay kit with JC-1, Beyotime, Wuhan, China). Flow cytometry was used to analysis the (ΔΨ) (EX = 488 nm; EM = 530 nm). Green fluorescence is detected through FL1; Red fluorescence is detected through FL2.

### Measuring the ATP level

The ATP detection kit was purchased from Biyuntian Biotechnology Research Institute in Wuhan of China. The simple steps of evaluating the ATP levels are as following: The regnant, samples and standards were prepared before setting blank holes, standard holes, and sample holes to be tested separately. Then, 50 mL of standard sample was added to the enzyme-linked immunosorbent assay (ELISA) plate with adding 40 mL of sample diluent and 10 mL of test sample (with a final dilution of 5 times) to the sample well, following gently shaking and mixing well, warm incubation( Seal the plate with a sealing film and incubate at 37 ℃ for 30 min) and washing 5 times ( every time includes carefully removing the sealing film, discarding the liquid, shaking dry, filling each well with washing solution, discarding washing solution and shaking to dry. Successively, add 50 mL of enzyme-linked immunosorbent assay reagent to each well excepting blank wells, then incubate and wash again before coloration. The coloration steps included adding 50 mL of chromogenic agent A to each well at first, then adding 50 mL of chromogenic agent B, gently shaking and mixing, and coloring at 37 ℃ in the dark for 15 min; After coloration, 50 mL of termination solution was added to each well for terminating the reaction and measuring the A value of each well in sequence at a wavelength of 450 nm.

### Quantitative reverse transcriptase PCR (qPCR)

The mRNA expression of the cells and pancreatic samples in all groups was evaluated using quantitative reverse transcriptase PCR and SYBR Green qPCR Master Mix. The primer sequences for different genes are listed in Table 1. The relative expression levels of different genes were calculated using the $2^{-\triangle\triangle Ct}$ method. The Ct values of β-actin in the same sample were used as an internal reference for standardization.

### Western blot

Pancreatic tissues and cells were lysed using radioimmunoprecipitation assay lysis buffer (1:100), crushed on ice, and cracked for 30 min. Proteins were collected by centrifugation at 12,000 rpm at 4℃ according to the manufacturer's instructions. Proteins were separated using 10% polyacrylamide gel electrophoresis and transferred onto polyvinylidene fluoride membranes. After sealing the membranes at room temperature for 1 h with a rapid sealing solution, they were cleaned using Tris-buffered saline with 0.1% Tween® 20 detergent (TBST) thrice. Antibodies against SIRT-1 (1:1,000), PGC-1α (1:500), NRF1 (1:500), TFAM (1:500), NLRP3 (1:1,000), caspase-1 (1:1,000), ASC (1:500), GSDMD (1:500), and β-actin (1:1,000) were added for overnight incubation at 4 ℃. Moreover, blots were cut prior to hybridisation with antibodies during blotting. After washing, the membranes were incubated with the secondary goat anti-rabbit immunoglobulin G (IgG) (1:10,000) at room temperature for 1 h. The membranes were then washed with TBST thrice. Protein bands were detected using the electrochemiluminescence method on a chemiluminescence imaging system. The results were analyzed using

the ImageJ (Full name: Image processing and Analysis in Java; Version Number: 2.0; URL Link: https://imagej.net/, USA).

### Statistical analyses

The SPSS ( Full name: IBM SPSS Statistical; Version Number :22.0; URL Link: https://www.ibm.com/products/spss-statistics, IBM, USA) software was used for statistical analysis. Data are expressed as mean ± standard deviation (SD). Comparisons between multiple groups were performed using one-way analysis of variance (ANOVA), and comparisons between two groups were performed using the least significant difference method. Differences were considered statistically significant at $P < 0.05$.

## Results

### RSV rescued pancreatic injury in SAP rats

To explore whether activating SIRT1 protected rats against SAP, we evaluated the classic pancreatic dysfunction marker (amylase and lipase) levels, pancreatic microcirculation, pancreatic D/W ratio, and pathological injury after RSV administration. Serum amylase and lipase are representative biochemical indicators of pancreatic function and both were remarkably increased in the SAP group; this increase was reversed after the RSV treatment. However, EX527 abolished the suppressive effect of RSV on the increases in amylase and lipase (Fig. 1A). Compared with the SAP group, the RSV group exhibited a relatively low D/W ratio, and EX527 suppressed this effect (Fig. 1B). PAS staining revealed ST-induced pathological changes, including widened pancreatic lobules, acini and intercellular spaces, swollen and necrotic acinar cells, and inflammatory cell infiltration with interstitial hemorrhage, in the pancreas. Predictably, RSV treatment lowered the grade of pancreatic damage, while EX527 aggravated it (Fig. 1C,D). Moreover, in comparison with the Ctrl group, the SAP group demonstrated significant pancreatic microcirculation impairment as demonstrated by the higher red blood cell flow and blood flow velocity, more numbers of pancreatic microvessels, higher erythrocyte rigidity and aggregation, and higher low, medium, and high shear viscosity of the whole blood, more expression of ET, NO, TXB-2、6-K-PGF-1α, higher ET/NO, and TXB-2/6-K-PGF-1α. As expected, RSV treatment improved the pancreatic microcirculation damage, while EX527 exacerbated pancreatic microcirculatory dysfunction

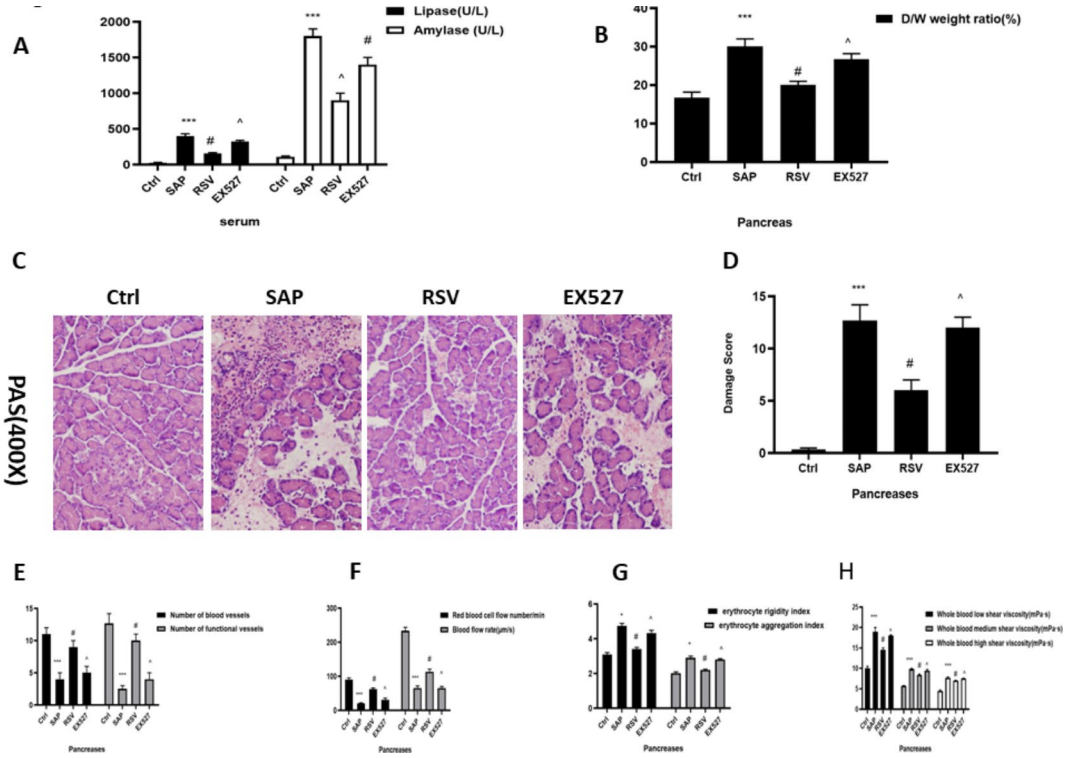


**Fig. 1**. The effect of RSV on pancreatic function of rats in SAP. (**A**) ELISA was used to evaluate the amylase and lipase activity in the serum; (**B**) Physical method was used to evaluate the wet/weight of pancreas; (**C**) Representative results for PAS staining histopathological morphology of pancreas; (**D**) Damage score of pancreas was evaluated by semi-quantitative analysis; (**E**) Microcirculatory Observation System Software was used to assess the red Blood Cell Flow and blood Flow rate; (**F**) Microcirculatory Observation System Software was used to assess the number of blood vessels and the number of functional blood vessels; (**G**) Blood rheology rapid detection instrument was used to assess the erythrocyte rigidity index, erythrocyte aggregation index; (**H**) Blood rheology rapid detection instrument was used to assess the low, medium, and high shear viscosity of whole blood; The data were represented as the mean ± S.D. ($n = 15$). ***$P < 0.001$ (SAP vs. Ctrl); #$P < 0.05$ (RSV vs. SAP); ^$P < 0.05$ (EX527 vs. RSV).

| Group | ET (pg/ml) | NO (pg/ml) | ET/NO | TXB2 (pg/ml) | 6-keto-PGF$_{1\alpha}$(pg/ml) | TXB2/6-keto-PGF$_{1\alpha}$ |
|---|---|---|---|---|---|---|
| Sham | 22. 55 ± 0.58 | 28.54 ± 0.62 | 0.79 ± 0. 03 | 10. 57 ± 0.59 | 11. 58 ± 0.29 | 0. 91 ± 0.06 |
| SAP | 129.35 ± 4.24*** | 90. 27 ± 1.31*** | 1. 43 ± 0. 07*** | 44.18 ± 0. 81*** | 28. 92 ± 1.13*** | 1. 52 ± 0.08*** |
| RSV | 85.17 ± 1.23# | 67. 48 ± 1.14# | 1. 26 ± 0. 04# | 23. 42 ± 0.62# | 18. 35 ± 0.79# | 1.27 ± 0.07# |
| EX527 | 105. 46 ± 3.98^ | 78. 84 ± 0.78^ | 1. 33 ± 0. 05^ | 41. 85 ± 0. 77^ | 25. 41 ± 1. 06^ | 1.64 ± 0.09^ |

**Table 2**. The effect of RSV on the vascular endothelium function in the SAP (, $n = 15$). Compared SAP group with Sham group, $^{***}P < 0.001$; Compared RSV group with SAP group, $^{\#}P < 0.05$; Compared EX527 group with RSV group, $^{\wedge}P < 0.05$.

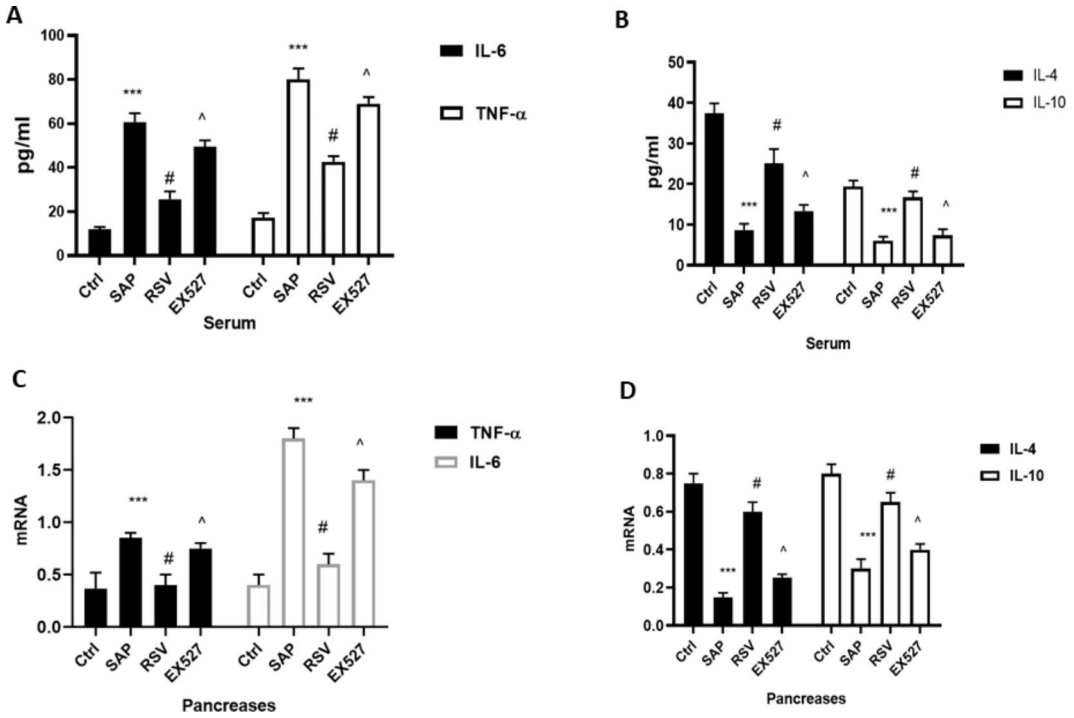


**Fig. 2**. The effect of RSV on inflammation in SAP. (**A**) ELISA was used to evaluate the expression of IL-6 and TNF-α in the serum; (**B**) ELISA was used to evaluate the expression of IL-4 and IL-10 in the serum; (**C**) RT-PCR was used to evaluate the mRNA level of IL-6 and TNF-α in the pancreas; (**D**) RT-PCR was used to evaluate the mRNA level of IL-4 and IL-10 in the pancreas; ($n = 15$). $^{***}P < 0.001$ (SAP vs. Ctrl); $^{\#}P < 0.05$ (RSV vs. SAP); $^{\wedge}P < 0.05$ (EX527 vs. RSV).

(Fig. 1E–H; Table 2) as confirmed higher red blood cell flow and blood flow velocity, more numbers of pancreatic microvessels, higher erythrocyte rigidity and aggregation, and higher low, medium, and high shear viscosity of the whole blood, more expression of ET, NO, TXB-2、6-K-PGF-1α, higher ratio of ET/NO, and TXB-2/6-K-PGF-1α in EX527 group than RSV group (Fig. 1E–H; Table 2). These results suggest that activation of SIRT1 can protect rats against ST-induced pancreatic impairment.

## Activating SIRT1 alleviated inflammation in SAP

The activation of inflammatory responses plays a vital role in SAP-induced cell death and pancreatic dysfunction[6]. Therefore, we examined the expression levels of IL-4, IL-10, TNF-α, and IL-6, which are representative anti-inflammatory and pro-inflammatory reaction indicators in SAP. As shown in Fig. 2, the serum and pancreatic levels of TNF-α and IL-6 were higher in the SAP group than in the Ctrl group, while IL-4 and IL-10 levels were lower. Treatment with RSV decreased the serum and pancreatic levels of TNF-α and IL-6 and increased those of IL-4 and IL-10. EX527 reversed the effect of RSV on inflammation in SAP as confirmed by higher expression levels of TNF-α and IL-6 and lower levels of IL-4 and IL-10 in the EX527 group than in the RSV group.

## SIRT1 activation attenuated pyroptosis by regulating the NLRP3 inflammasome

Activating the NLRP3 inflammasome-pyroptosis axis can promote strong inflammatory responses and cell death in SAP[6,7]. Therefore, we measured the levels of NLRP3 inflammasome-pyroptosis axis-associated proteins. The expression levels of NLRP3, Caspase-1, and GSDMD, IL-1β, ASC, and IL-18 were all higher in the SAP group than in the Ctrl group, while RSV significantly reduced their expression. EX527, a SIRT1 inhibitor, reversed the

effect of RSV on NLRP3 inflammasome pathway-mediated pyroptosis as demonstrated higher expression levels of NLRP3, Caspase-1, and GSDMD, IL-1β, ASC, and IL-18 in the EX527 group than RSV group (Fig. 3).

## RSV inhibited the translocation of mtDNA in SAP

Translocation of mtDNA from the mitochondria to the cytosol can serve as a trigger for the activation of the NLRP3 inflammasome and an effector for pathological processes[26]. We observed ST decreased the amount of mitochondrial mtDNA and increased that in the cytosol (Fig. 4A,B). Notably, RSV can alleviate ST-induced mtDNA translocation as confirmed more amount of mitochondrial mtDNA and less cytosolic mtDNA in the RSV group than in the SAP group (Fig. 4A,B). However, EX527 can inhibit the effect of RSV translocation of mtDNA in SAP. These results indicate that activating SIRT1 can suppress ST-induced translocation of mtDNA to the cytosol.

## RSV improved mitochondrial dysfunction in SAP

The excessive production of mitochondrial ROS can cause mitochondrial damage, which promotes mtDNA translocation[27]. We measured the mitochondrial ROS and ATP contents, ΔΨm, and MDA, SOD, and GSH levels, which are classical indicators of mitochondrial function. ST significantly induced increased levels of mitochondrial ROS and MDA (Fig. 5C,D), while decreasing SOD and GSH activity, ΔΨm, and ATP content (Fig. 5). RSV treatment down-regulated the expression of mitochondrial ROS and MDA, while upregulating the activities of SOD and GSH, the ΔΨm, and ATP content. However, EX527 antagonized the effect of RSV on mitochondrial function in SAP. Therefore, our results suggest that the activation of SIRT1 can improve ST-induced mitochondrial damage.

## RSV promoted mitochondrial biogenesis by regulating PGC-1α/ NRF1/TFAM in SAP

Mitochondrial biogenesis is an important process for maintaining cellular homeostasis by producing new mitochondria, and its activation is mainly dominated by PGC-1α[11,12]. Moreover, NRF1 and TFAM are downstream proteins of PGC-1α[13,14]. The results showed that PGC-1α, NRF1, and TFAM levels were all significantly reduced at both the gene and protein levels in the pancreas of the SAP group, thus indicating that mitochondrial biogenesis was seriously impaired. RSV can facilitate mitochondrial biosynthesis by increasing the protein and gene expression levels of PGC-1α, NRF1, and TFAM, while antagonizing SIRT1 via EX527 can reverse the influence of RSV on mitochondrial biosynthesis in SAP (Fig. 6A,B). Similar experimental results

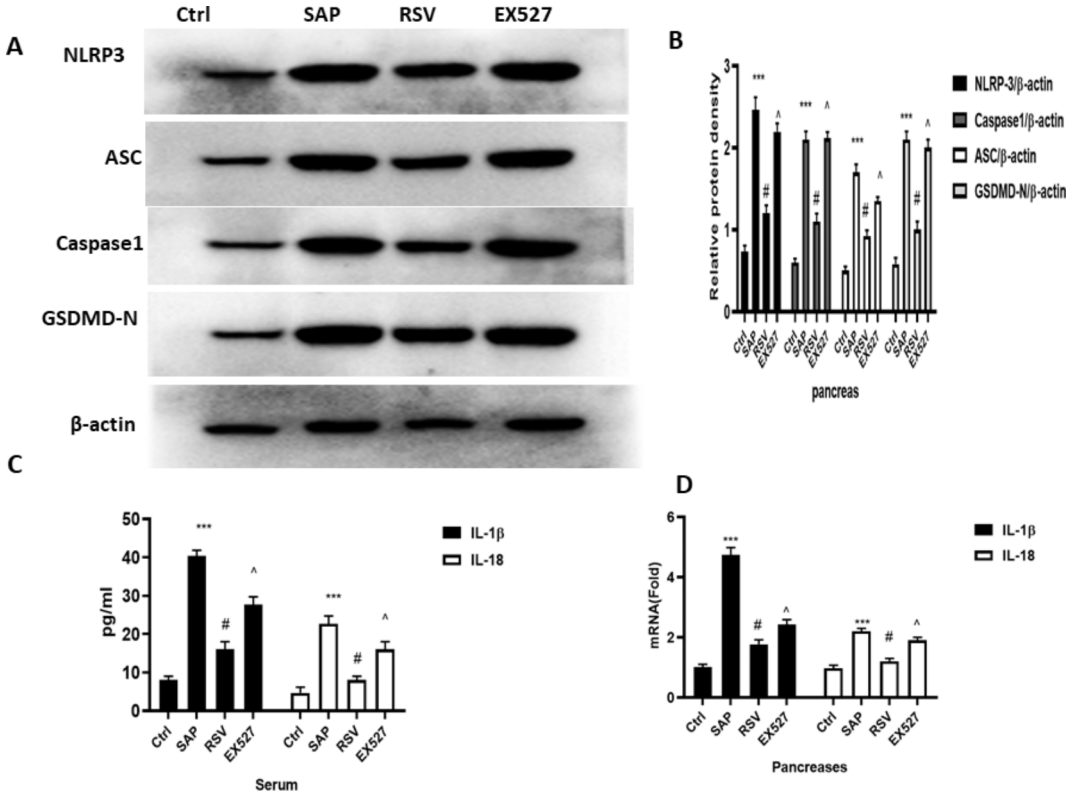


**Fig. 3**. The effect of RSV on NLRP3 inflammasomes- pyroptosis axis on rats in SAP. (**A**) Typical result for Western blotting analysis NLRP3, ASC, Caspase1 and GSDMD in the pancreas. (**B**) The NLRP3, ASC, Caspase1 and GSDMD expression of pancreas was assessed by semi-quantitative analysis; (**C**) ELISA was used to evaluate the expression of IL-1β and IL-18 in the serum; (**D**) RT-PCR was used to evaluate the m RNA level of IL-1β and IL-18 in the pancreas; the data were represented as the mean ± S.D. ($n = 15$).$^{***}P < 0.001$ (SAP vs. Ctrl ); $^{\#}P < 0.05$ (RSV vs. SAP); $^{\wedge}P < 0.05$ (EX527 vs. RSV).

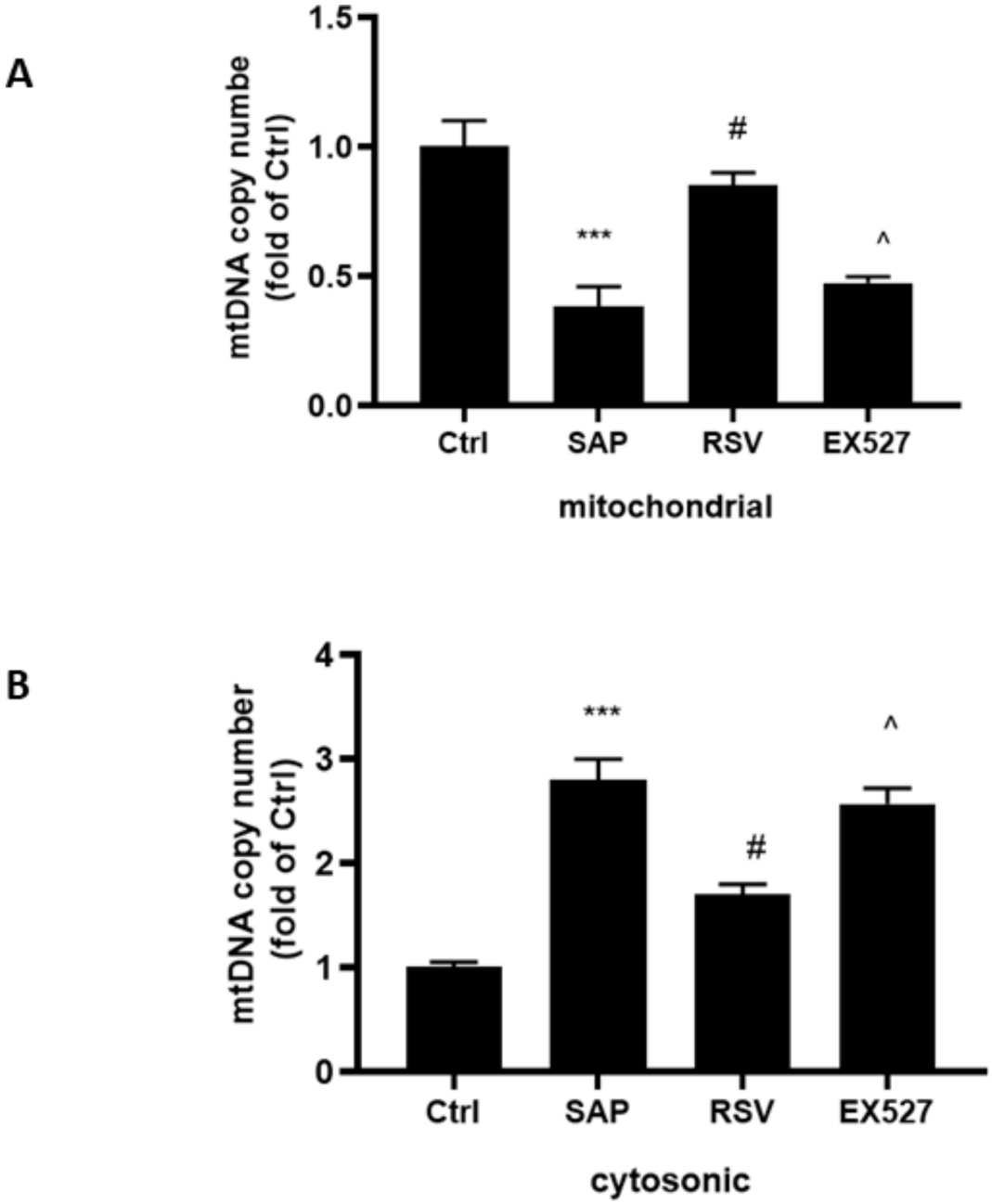


**Fig. 4**. The effect of RSV on translocation of mtDNA on rats in SAP. (**A**) RT-PCR was used to evaluate the level of mitochondria mtDNA in the pancreas; (**B**) RT-PCR was used to evaluate the level of cytosolic mtDNA in the pancreas; The data were represented as the mean ± S.D. ($n = 15$). $^{***}P < 0.001$ (SAP vs. Ctrl ); $^{\#}P < 0.05$ (RSV vs. SAP); $^{\wedge}P < 0.05$ (EX527 vs. RSV).

were also obtained in cell experiments (Fig. 7G–L). To further confirm whether RSV can reduce the activation of the NLRP3 inflammasome via mitochondrial biogenesis, we employed AR42J cells to establish a model of SAP by culturing them with ST in vitro. AR42J cells were preconditioned with a PGC-1α inhibitor (SR-18292), which promoted PGC-1α acetylation, as well as ST. When PGC-1α expression was repressed, NRF1 and TFAM expression was reduced even after RSV treatment, which increased the translocation of mtDNA (Fig. 6C–G). Similarly, the activities of SOD and GSH and ΔΨm and ATP content in the mitochondria were all reduced in AR42J cells after treatment with SR-18,292, while MDA and ROS levels increased (Fig. 6H–K). These results indicate that SR-18,292 can offset the protective effect of RSV in AR42J cells under ST stimulation.

We also attempted to identify the relationship between mitochondrial biogenesis and pyroptosis in SAP. When preconditioned with SR-18,292, the expression levels of pyroptosis-associated NLRP3, caspase-1, GSDMD-N, IL-1β, ASC, and IL-18 were distinctly augmented (Fig. 6L–O). In addition, the suppressive effect of RSV on the aforementioned proteins and genes was reversed. Moreover, we also observed an increase in the

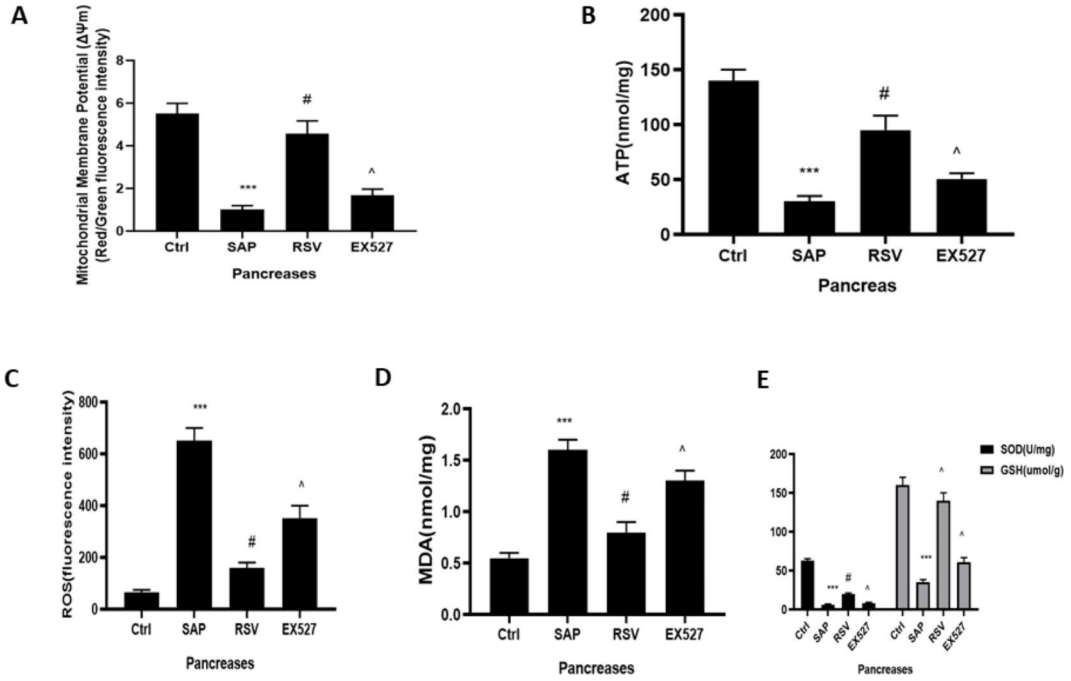


**Fig. 5**. The effect of RSV on Mitochondrial function and oxidative stress on rats in SAP. (**A**) Mitochondrial membrane potential detection kit of JC-1 was used to examine the mitochondrial membrane potential in the acinar cells; (**B**) The ATP assay kit was used to evaluate the content of ATP in the acinar cells; (**C**) MitoSOX was used to test the level of ROS in the mitochondrial; (**D**) The MDA levels and (**E**) SOD and GSH activity of acinar cells were detected to evaluate the oxidative stress. The data were represented as the mean ± S.D. ($n = 15$). $^{***}P < 0.001$ (SAP vs. Ctrl); $^{\#}P < 0.05$ (RSV vs. SAP); $^{\wedge}P < 0.05$ (EX527 vs. RSV).

cell viability of AR42J cells under the RSV treatment after ST stimulation (Fig. 6P). However, SR-18,292 can counteract the effect of RSV on cell viability in AR42J cells after ST stimulation. These results imply that RSV can regulate NLRP3 inflammasome-mediated pyroptosis by suppressing the activation of mtDNA in a PGC-1α-dependent manner.

### RSV increased PGC-1α activity via SIRT1 in SAP

RSV not only stimulates the expression of PGC-1α at the mRNA and protein levels via the activation of SIRT1 but also facilitates the deacetylation and activity of PGC-1α[15,16]. Therefore, we investigated PGC-1α acetylation and SIRT1 activity in SAP. Similar experiments were also performed on cultured AR42J cells. We observed, when compared with the SAP group, RSV-treated rats and cell had significantly high SIRT1 expression and activity (Fig. 7) and low ratios of acetylated nuclear PGC-1α to total nuclear PGC-1α; this indicates that the activity of SIRT1 and PGC-1α were both increased. In contrast, EX527 reversed the effect of RSV in SIRT1 activation and the acetylation and activity of PGC-1α (Fig. 7A–K).

To investigate whether the protective effect of RSV on mitochondrial biogenesis was mediated by PGC-1α and SIRT1, we coinfected AR42J cells with an adenovirus, which overexpressed PGC-1α or SIRT1, as well as a specific siRNA directed against either SIRT1 or PGC-1α. This effectively decreased the levels of endogenous SIRT1 while simultaneously maintaining high PGC-1α expression. Notably, PGC-1α knockdown led to increases in cell viability and the expression levels of PGC-1α, NRF-1, and TFAM (induced by RSV) (Fig. 7L–N). Moreover, in AR42J cells, which overexpressed PGC-1α owing to transfection, RSV treatment led to significant increases in cell viability and the expression of PGC-1α, NRF-1, and TFAM, further confirming that the effects of RSV on SAP are PGC-1α-dependent.

To further strengthen our finding that RSV activates PGC-1α independently of SIRT1, we compared the expression of PGC-1α in AR42J cells, which overexpressed SIRT1 or a SiRNA against SIRT1. The results showed that RSV induced increased PGC-1α acetylation and reduced SIRT1, PGC-1α, NRF-1, and TFAM expression levels in siRNA-SIRT1 cells, under ST stimulation. Notably, in AR42J cells, which overexpressed SIRT1 under ST stimulation, RSV significantly reduced PGC-1α acetylation and increased the expression of SIRT1, PGC-1α, NRF-1, and TFAM (Fig. 7O–T). These results indicate that RSV treatment gives rise to PGC-1α deacetylation and regulation of PGC-1α target genes in AR42J cells and rat models of SAP.

*The structure of resveratrol (Fig. 8)*

## Discussion

SAP is a common disease known for its high mortality and morbidity[1]. To date, no satisfactory treatment measures are available[1–,2]. Therefore, it is essential to explore novel drugs and targets for SAP therapy. Numerous studies

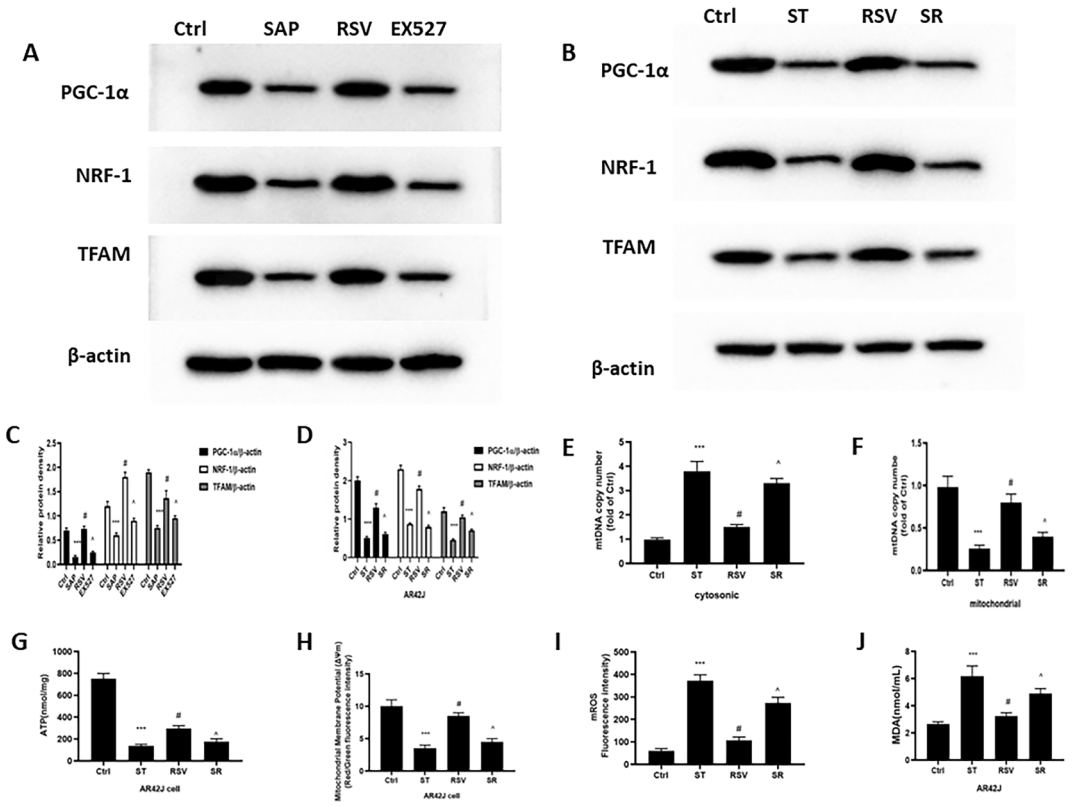


**Fig. 6**. The effect of RSV in mitochondrial biogenesis on rats and cell in SAP. (**A**) Typical result for Western blotting analysis PGC-1α, NRF1 and TFAM in the pancreas. (**B**) The PGC-1α, NRF1 and TFAM expression of pancreas was assessed by semi-quantitative analysis; (**C**) Typical result for Western blotting analysis PGC-1α, NRF1 and TFAM in the AR42Jcell. (**D**) The PGC-1α, NRF1 and TFAM expression of pancreas was assessed by semi-quantitative analysis; (**E**) RT-PCR was used to evaluate the level of cytosolic mtDNA in the AR42J cell; (**F**) RT-PCR was used to evaluate the level of mitochondria mtDNA in the AR42J cell; (**G**) The ATP assay kit was used to evaluate the content of ATP in the AR42J cell; H: Mitochondrial membrane potential detection kit of JC-1 was used to examine the mitochondrial membrane potential in the AR42J cell; (**I**) MitoSOX was used to test the level of ROS in the mitochondrial of AR42J cell; (**J**) The MDA levels and (**K**) SOD and GSH activity of AR42J were detected to evaluate the oxidative stress; (**L**) Typical result for Western blotting analysis NLRP3, ASC, Caspase1 and GSDMD in the AR42J cell. (**M**) The NLRP3, ASC, Caspase1 and GSDMD expression of AR42J cell was assessed by semi-quantitative analysis; (**N**) RT-PCR was used to evaluate the mRNA level of IL-1β and IL-18 in the AR42J cell; (**O**) ELISA was used to evaluate the expression of IL-1β and IL-18 in the supernatant; (**P**) CCK-8 kit was use to examine the cell viability of AR42J cell. The data were represented as the mean ± S.D. ($n = 15$). $^{***}P < 0.001$ (SAP vs. Ctrl); $^{\#}P < 0.05$ (RSV vs. SAP); $^{\wedge}P < 0.05$ (EX527 vs. RSV); The data were represented as the mean ± S.D. ($n = 3$). $^{***}P < 0.001$ (ST vs. Ctrl); $^{\#}P < 0.05$ (RSV vs. ST); $^{\wedge}P < 0.05$ (SR vs. RSV);

have shown that natural medicinal plants and their active ingredients can improve the symptoms of pancreatic diseases and that the aseptic and systemic inflammatory responses play important roles in the occurrence and development of SAP[3-4.14]. Thus, RSV, a typical SIRT1 agonist with outstanding anti-inflammatory properties, has gained our attention[14,15]. Our results showed that RSV treatment could significantly alleviate pancreatic pathological injury, improve the pancreatic microcirculation impairment (blood, and the ratio of ET/NO, and TXB-2/6-K-PGF-1α, which are commonly used to evaluate pancreatic microcirculation function) and down-regulate D/W ratio, decrease amylase and lipase levels in SAP, and increase the expression levels of anti-inflammatory factors (IL-4 and IL-10) while reducing those of pro-inflammatory factors (IL-6 and TNF-α). Accordingly, EX, a SIRT1 inhibitor, can antagonize the effects of RSV on SAP. Our findings further suggested that the protective effect of RSV on SAP was achieved by suppressing SIR1-dependent inflammation.

Pyroptosis, a pro-inflammatory form of lytic cell death, can release inflammatory factors, eliminate pathogens, and is of great significance for maintaining normal body balance[6,7]. However, excessive cell pyroptosis can lead to marked cell death, exacerbate the inflammatory response process, and cause severe organ damage[6]. Notably, the classic pathways of pyroptosis include caspase-1 activation, membrane pore formation, and release of cellular contents[6,7]. The activation of caspase1 requires the involvement of the NLRP3 inflammatory complex composed of NLRP3, ASC, and pro-caspase-1. In addition, NLRP3 is considered to be a receptor for intracellular damage and is capable of responding to pathogen-related molecular patterns and damage-related molecular patterns[6,7]. Activated NLRP3 transmits signals to downstream ASC, which can act as a bridge for recruiting pro caspase-1,

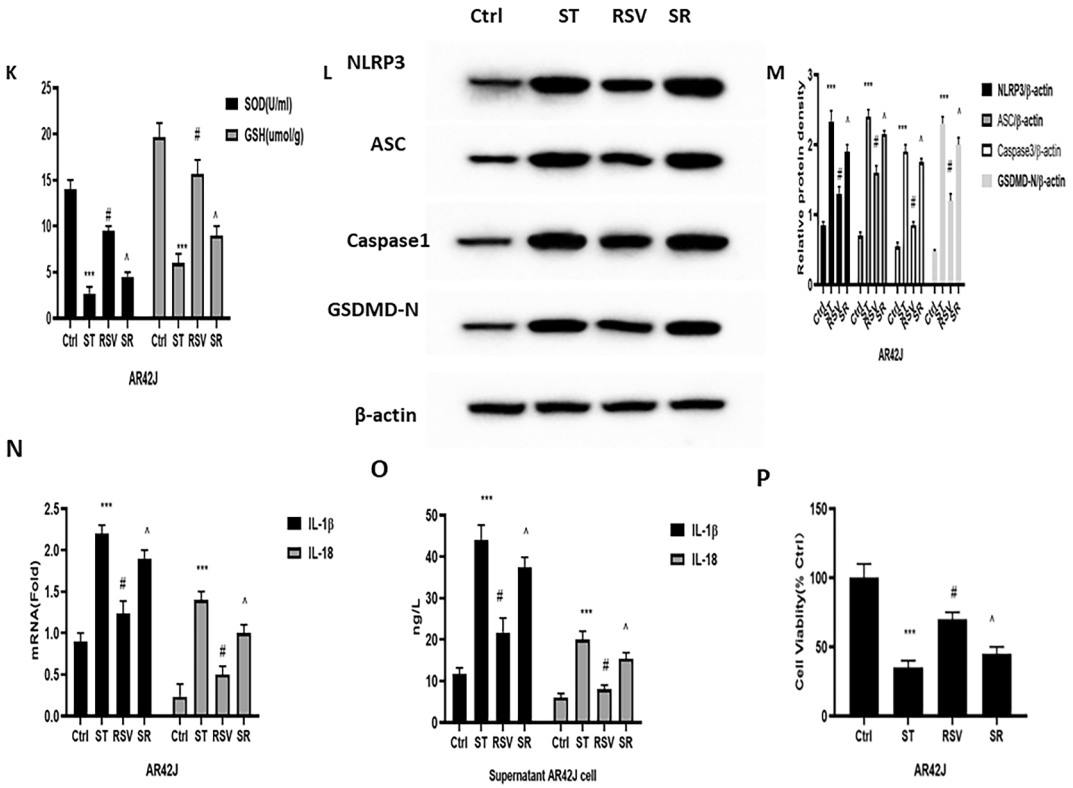


**Figure 6.** (continued)

forming an inflammatory complex, and cleaving pro-caspase-1 into active caspase-1. Activating caspase-1 allows for GSDMD cleavage, thus recruiting and cleaving the precursors of IL-18 and IL-1β to active IL-18 and IL-1β[6,7]. Moreover, cleaved GSDMD can recognize and bind to the corresponding phospholipid protein on cell membranes to form membrane pores, inducing pyroptosis initiation[6,7]. Notably, the membrane pores formed by pyroptosis can activate IL-1 β and IL-18 to be released outside of cells, which induces and exacerbates systemic reactions[6,7]. Previous studies have confirmed that pyroptosis derived from NLRP3 activation exacerbates pancreatitis and that IL-1β is considered to be the main cytokine causing early inflammatory spreading in SAP[6,7]. In this study, RSV significantly suppressed SAP-induced increases in NLRP3, Caspase-1, and GSDMD, IL-1β, ASC, and IL-18 expression. EX abolished the influence of RSV on the expression of the aforementioned proteins. Moreover, studies have confirmed that caspase 1 inhibitors and NLRP3 suppressors can decrease the expression of GSDMD, IL-1β, ASC, and IL-18 in SAP. Thus, our results indicated the suppressive effect of RSV in inflammation, which was mediated by inhibiting the NLRP3 inflammasome-pyroptosis axis via SIRT1 activation.

Notably, previous studies have confirmed that SIRT1 is closely associated with mitochondrial function and that mitochondrial damage can trigger the activation of the NLRP3 inflammasome[28]. Moreover, mitochondrial dysfunction, the release of mitochondrial ROS (mtROS), and the oxidation and translocation of mtDNA are critical upstream steps in the activation of the NLRP3 inflammasome[28,29]. In addition, mitochondrial damage may promote the changes in ΔΨm, ATP synthesis, mtROS translocation, oxidative stress and antioxidant processes, and the oxidation and removal of mtDNA, which are typically observed in mitochondrial dysfunction[28,29]. In this study, SAP significantly decreased the ΔΨm, ATP content, and antioxidant stress kinase (SOD and GSH) activity, while increasing the levels of a pro-oxidant stress kinase (MDA) and mROS, along with augmenting the migration of mtDNA to the cytosol. Our results further showed that RSV can reverse these SAP-induced effects, while EX527 can abate the protective effect of RSV on the mitochondria in SAP. These results imply that the inhibitory effect of RSV on NLRP3 inflammasome activation in SAP depends on decreasing mitochondrial damage and improving mitochondrial dysfunction via the activation of SIRT1.

The mitochondria are dynamic organelles and undergo biosynthesis, fusion, division, and autophagy to maintain energy supply to the body[8]. Mitochondrial biosynthesis is a process of regenerating fully functional mitochondria based on existing mitochondria. In addition, mitochondrial biogenesis is a critical step for restoring mitochondrial homeostasis via the generation of new mitochondria and normalization of mitochondrial function[8–10]. Notably, mitochondrial dysfunction can be relieved via mitochondrial biogenesis[9,10]. Thus, we paid special attention to the regulatory factors of mitochondrial biogenesis. PGC-1α, a well-known core molecule in initiating mitochondrial biogenesis, has attracted considerable research interest[11]. PGC-1α can regulate NRF1 expression by monitoring various mtDNA-encoded mitochondrial genes[11,12]. NRF-1 can sensitize the expression of nuclear genes, which are necessary for biogenesis and mitochondrial function, including heme biosynthetase, mitochondrial respiratory complex subunits, and regulatory factors associated

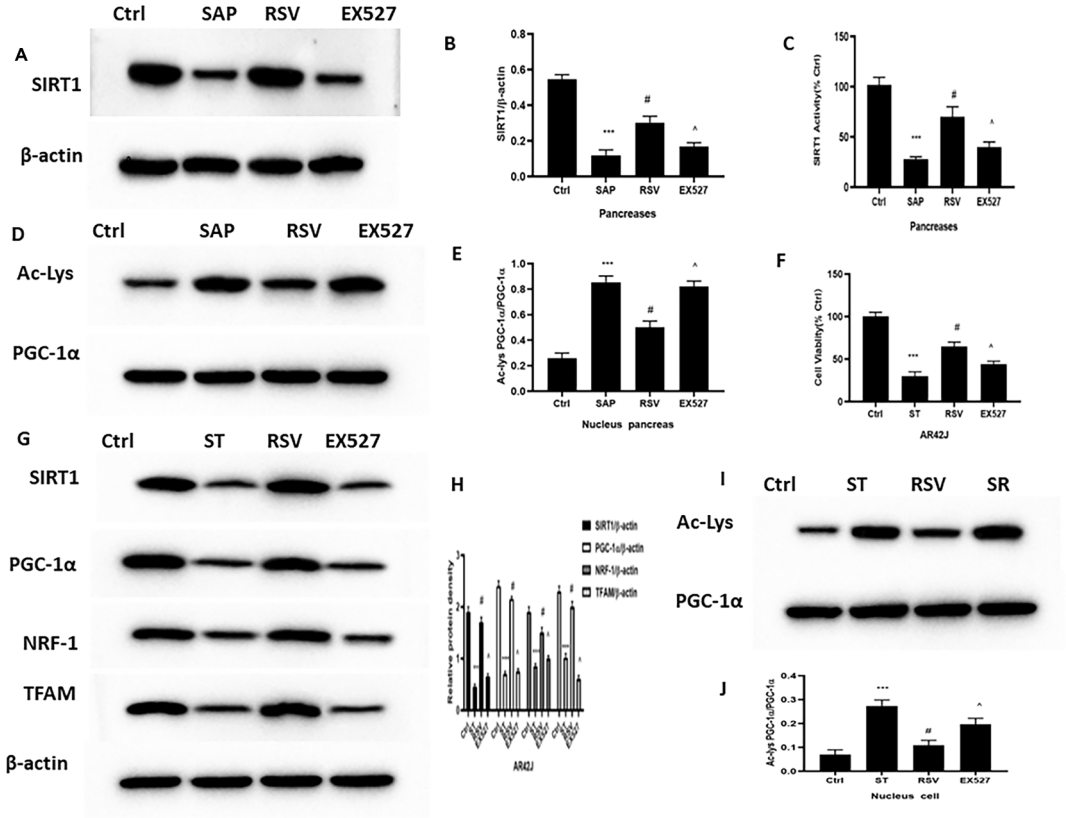


**Fig. 7**. The effect and mechanism of RSV on PGC-1α in SAP. (**A**) Typical result for Western blotting analysis SIRT1 in the pancreas. (**B**) The SIRT1 expression of pancreas was assessed by semi-quantitative analysis; (**C**) The SIRT1 kit was used to the activity of SIRT1 deacetylase in the pancreas; (**D**) The co-immunoprecipitation was used to evaluate the interaction of PGC-1α and Ace-lys in the nucleus in the pancreas; (**E**) The interaction of PGC-1α and Ace-lys in the nucleus of pancreas was assessed by semi-quantitative analysis; (**F**) CCK-8 kit was use to examine the cell viability of AR42J cell; (**G**) Typical result for Western blotting analysis PGC-1α, NRF1 and TFAM in the AR42Jcell. (**H**) The PGC-1α, NRF1 and TFAM expression of pancreas was assessed by semi-quantitative analysis; (**I**) The co-immunoprecipitation was used to evaluate the interaction of PGC-1α and Ace-lys in the nucleus of AR42J cell; (**J**) The interaction of PGC-1α and Ace-lys in the nucleus of AR42J cell was assessed by semi-quantitative analysis; (**K**) The SIRT1 kit was used to the activity of SIRT1 deacetylase in the AR42J cell; (**L**) Typical result for Western blotting analysis PGC-1α, NRF1 and TFAM in the AR42Jcell. (**M**) The PGC-1α, NRF1 and TFAM expression of AR42J cell was assessed by semi-quantitative analysis; (**N**) CCK-8 kit was use to examine the cell viability of AR42J cell; (**O**) Typical result for Western blotting analysis SIRT1, PGC-1α, NRF1 and TFAM in the AR42Jcell. (**P**) The SIRT1, PGC-1α, NRF1 and TFAM expression of AR42J cell was assessed by semi-quantitative analysis; (**Q**) CCK-8 kit was use to examine the cell viability of AR42J cell; (**R**) The SIRT1 kit was used to the activity of SIRT1 deacetylase in the AR42J cell; (**S**) The co-immunoprecipitation was used to evaluate the interaction of PGC-1α and Ace-lys in the nucleus of AR42J cell; (**T**) The interaction of PGC-1α and Ace-lys in the nucleus of AR42J cell was assessed by semi-quantitative analysis; The data were represented as the mean ± S.D. ($n = 15$). $^{***}P < 0.001$ (SAP vs. Ctrl); $^{\#}P < 0.05$ (RSV vs. SAP); $^{\wedge}P < 0.05$ (EX527 vs. RSV); The data were represented as the mean ± S.D. ($n = 3$). $^{***}P < 0.001$ (RSV vs. SiRNA-PGC-1α); $^{\#}P < 0.05$ (RSV vs. Plasmid-PGC-1α); $^{***}P < 0.001$ (RSV vs. SiRNA-SIRT1); $^{\#}P < 0.05$ (RSV vs. Plasmid-SIRT1).

with DNA replication and mitochondrial transcription[11,12]. Moreover, NRF-1 can also facilitate mitochondrial gene transcription by activating TFAM. Notably, TFAM, a nuclear coding protein located in the cytoplasm, can mitigate into the mitochondria and is the principal transcriptional factor for maintaining the mitochondria[11,12]. TFAM actively takes part in the structural synthesis of mtDNA and boosts mitochondrial biogenesis. When TFAM is lost, the structure and function of mtDNA will be damaged, as shown by severe defects in respiratory chain function and decreased mtDNA copy numbers[12]. High TFAM expression can remarkably ameliorate structural damage and dysfunction in the mitochondria, thereby alleviating disease symptoms[11,12]. Currently, some studies have confirmed that upregulating the expression levels of PGC-1α, NRF-1, and TFAM can alleviate SAC by promoting mitochondrial biogenesis. Both in vivo and in vitro experiments in our study have shown that RSV can increase the expression levels of PGC-1α, NRF-1, and TFAM, as well as mitochondrial mtDNA levels. Additionally, EX can antagonize the aforementioned influence of RSV on SAP, indicating that the activation of SIRT1 by RSV advances mitochondrial biogenesis by activating PGC-1α/NRF-1/TFAM signaling in SAP.

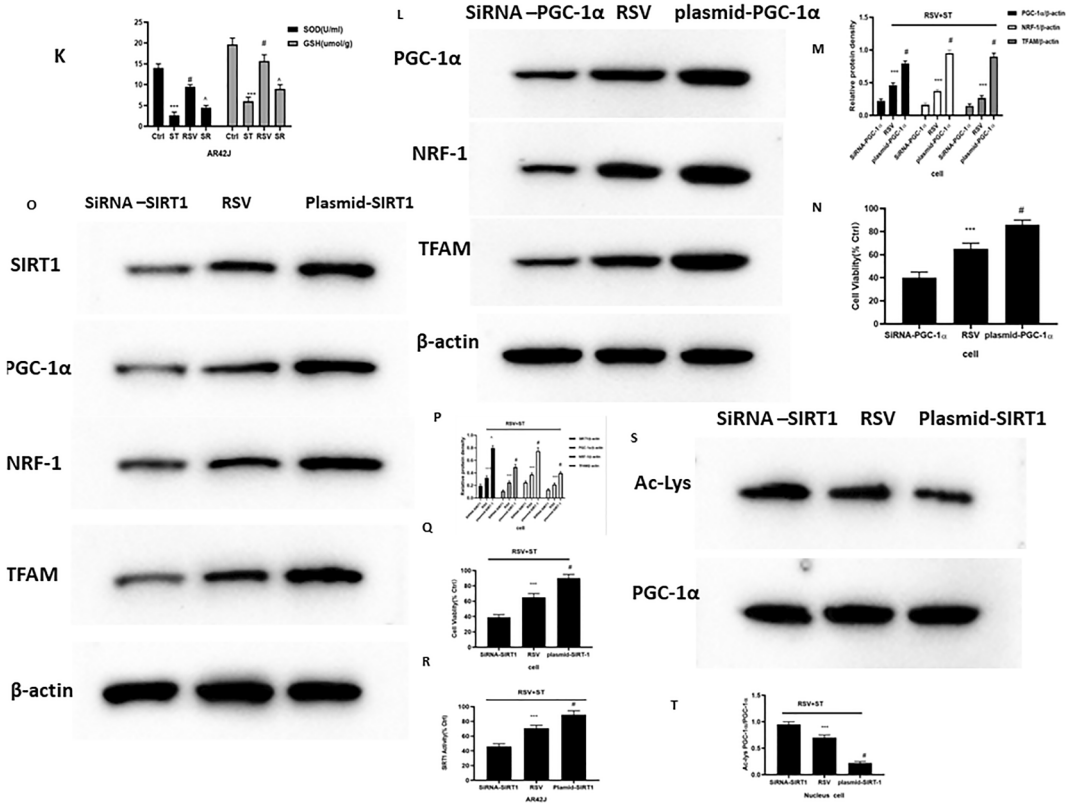


**Figure 7.** (continued)

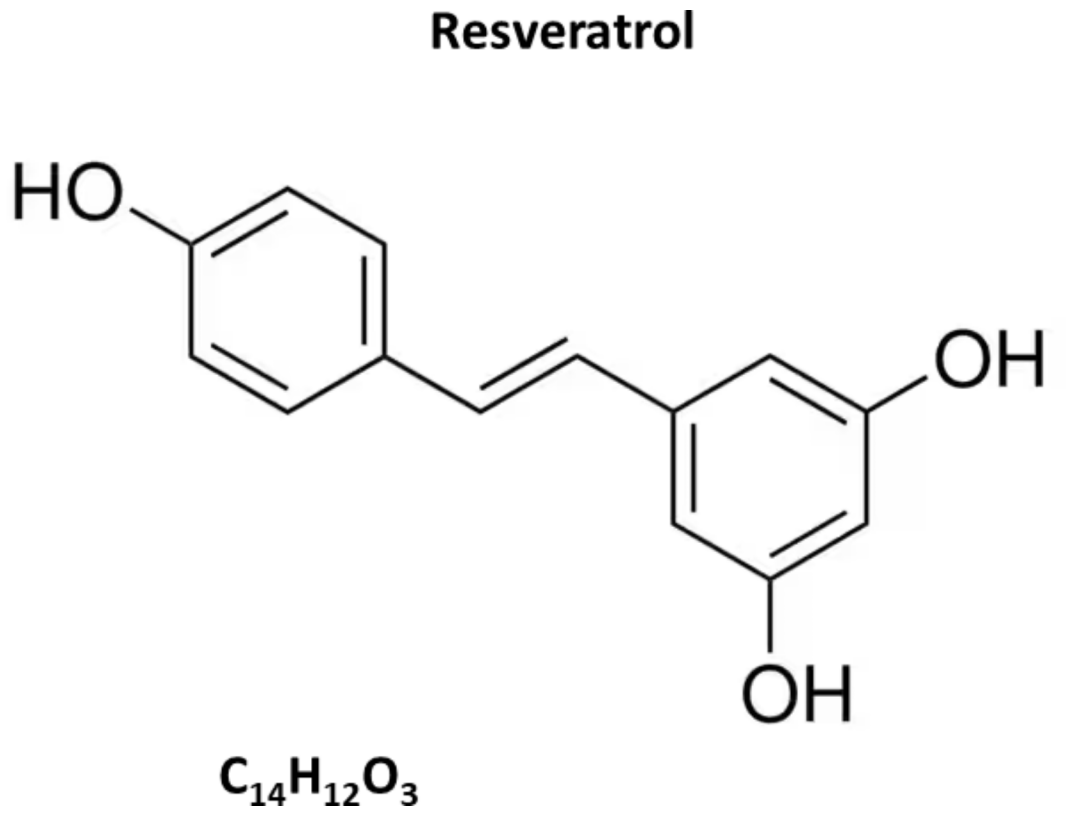


**Fig. 8**. The structure of RSV.

Notably, in vivo research also found that suppressing PGC-1α via SR (a PGC-1α inhibitor) or siRNA PGC-1α both impaired the influences of RSV on cell viability, mitochondrial biogenesis-associated protein expression, mitochondrial function, and the NLRP3 inflammasome-pyroptosis axis. Moreover, PGC-1α overexpression can restore and promote the abovementioned protective effect of RSV in an AR42J cell model of SAP. The results clearly suggest that the beneficial effect of RSV in mitochondrial dysfunction is dependent on PGC-1α-mediated mitochondrial biogenesis in SAP.

The activity of PGC-1α is regulated by various post-translational modifications and proteins, including GSK-3β, adenylate activated protein kinase AMPK, histone acetyltransferase GCN5, and nicotinamide dependent deacetylase SIRT1[11,27]. Among them, SIRT1 is of particular interest. SIRT1 is mainly located in the nucleus and can catalyze nuclear PGC-1α deacetylation to prevent ubiquitination degradation, thus maintaining high expression levels of PGC-1α in the nucleus and mediating mitochondrial biogenesis[10,11]. In this study, RSV increased the activity and expression of SIRT1, decreased nuclear PGC-1α acetylation, and upregulated cell viability and the expression levels of PGC-1α, NRF-1, and TFAM. EX or siRNA SIRT1 suppressed the effect of RSV, while overexpressing SIRT1 restored and promoted the aforementioned protective effect of RSV in an AR42J cell model of SAP. These results indicate that the promotion of RSV-induced mitochondrial biogenesis in SAP is via deacetylation of PGC-1α in the nucleus in a SIRT1-dependent manner.

In conclusion, in this study, we revealed the important role of mitochondrial dysfunction in the activation of the NLRP3 inflammasome-pyroptosis axis during the pathogenesis of SAP, as well as possible mechanisms of RSV in improving mitochondrial dysfunction. We showed that the protective effects of RSV rely on activating PGC-1α/NRF-1/TFAM-mediated mitochondrial biosynthesis in a SIRT1-dependent manner in SAP. Our study provides strong evidence that targeting the SIRT1/PGC-1α pathway may be a promising therapeutic strategy for SAP.

## Data availability

The data supporting the findings of this study are available from the corresponding author upon request.

Received: 8 February 2024; Accepted: 16 October 2024
Published online: 31 October 2024

## References

1. Mederos, M. A., Reber, H. A. & Girgis, M. D. Acute pancreatitis: a review. *JAMA*. **325** (4), 382–390 (2021).
2. Lankisch, P. G., Apte, M. & Banks, P. A. Acute pancreatitis. *Lancet*. **386** (9988), 85–96 (2015).
3. Gliem, N., Ammer-Herrmenau, C., Ellenrieder, V. & Neesse, A. Management of severe acute pancreatitis: an update. *Digestion*. **102** (4), 503–507 (2021).
4. Zerem, E. Treatment of severe acute pancreatitis and its complications. *World J. Gastroenterol.* **20** (38), 13879–13892 (2014).
5. Hines, O. J. & Pandol, S. J. Management of severe acute pancreatitis. *BMJ*. **367**, l6227. https://doi.org/10.1136/bmj.l6227 (2019).
6. Gao, L. et al. Acinar cell NLRP3 inflammasome and gasdermin D (GSDMD) activation mediates pyroptosis and systemic inflammation in acute pancreatitis. *Br. J. Pharmacol.* **178** (17), 3533–3552 (2021).
7. Lu, Y. et al. HDL inhibits pancreatic acinar cell NLRP3 inflammasome activation and protect against acinar cell pyroptosis in acute pancreatitis. *Int. Immunopharmacol.* **125** (Pt A), 110950 (2023).
8. Monzel, A. S., Enríquez, J. A. & Picard, M. Multifaceted mitochondria: moving mitochondrial science beyond function and dysfunction. *Nat. Metab.* **5** (4), 546–562 (2023).
9. Zhang, Y. et al. ALDH2 attenuates myocardial pyroptosis through breaking down Mitochondrion-NLRP3 inflammasome pathway in septic shock. *Front. Pharmacol.* **14**, 1125866 (2023).
10. Pérez, S. et al. Obesity causes PGC-1α deficiency in the pancreas leading to marked IL-6 upregulation via NF-κB in acute pancreatitis. *J. Pathol.* **247** (1), 48–59 (2019).
11. Budai, A. et al. Mitochondrial function after associating liver partition and portal vein ligation for staged hepatectomy in an experimental model. *Br. J. Surg.* **106** (1), 120–131 (2019).
12. Dong, Y. Z., Li, L., Espe, M., Lu, K. L. & Rahimnejad, S. Hydroxytyrosol attenuates hepatic Fat Accumulation via activating mitochondrial Biogenesis and Autophagy through the AMPK pathway. *J. Agric. Food Chem.* **68** (35), 9377–9386 (2020).
13. Chen, J.-W., et al. mito-TEMPO attenuates oxidative stress and mitochondrial dysfunction in noise-Induced hearing loss via maintaining TFAM-mtDNA Interaction and mitochondrial Biogenesis. *Front. Cell. Neurosci.* **8**, 16803718 (2022).
14. Malaguarnera Influence of Resveratrol on the Immune response. *Nutrients*. **11** (5), 946 (2019).
15. Yang, M. et al. Protective effect of resveratrol on mitochondrial biogenesis during hyperoxia-induced brain injury in neonatal pups. *BMC Neurosci.* **24** (1), 27 (2023).
16. Ghosh, J. et al. Cigarette smoke toxins-Induced mitochondrial dysfunction and pancreatitis involves aryl hydrocarbon receptor mediated Cyp1 gene expression: Protective effects of Resveratrol. *Toxicol. Sci.* **166** (2), 428–440 (2018).
17. Song, Q. et al. Gabexate mesylate-poloxamer 407 conjugate alleviates sodium taurocholate-induced severe acute pancreatitis in an optimized rat model. *Dig. Dis. Sci.* **68** (1), 138–146 (2023).
18. Liu, D. L., Song, G. D., Ma, Z. L. & Song, Z. S. Efficacy of resveratrol in treating rat models with severe acute pancreatitis. *Jiangsu Med. J.* **46** (4), 325–328 (2020).
19. Rong, Y. et al. Resveratrol suppresses severe Acute Pancreatitis-Induced Microcirculation disturbance through Targeting SIRT1-FOXO1 Axis. *Oxid. Med. Cell. Longev.* **2021**, 8891544 (2021).
20. Wang, J. et al. Amelioration of experimental acute pancreatitis with Dachengqi Decoction via regulation of necrosis-apoptosis switch in the pancreatic acinar cell. *PLoS One*. **7**, e40160 (2012).
21. Changsheng, Y. Endoplasmic reticulum stress promotes caspase-1-dependent acinar cell pyroptosis through the PERK pathway to aggravate acute pancreatitis. *Int. Immunopharmacol.* **120**, 110293. https://doi.org/10.1016/j.intimp.2023.110293 (2023).
22. Ji, L. et al. Hydrogen sulphide exacerbates acute pancreatitis by over-activating autophagy via AMPK/mTOR pathway. *J. Cell. Mol. Med.* **20** (12), 2349–2461 (2016).
23. Ji, L. et al. Hypoxia-inducible factor-1α knockdown plus glutamine supplementation attenuates the predominance of necrosis over apoptosis by relieving cellular energy stress in acute pancreatitis. *Oxid. Med. Cell. Longev.* **43**, 636–672 (2019).
24. Sebai, H. et al. Protective effect of resveratrol against LPS-induced extracellular lipoperoxidation in AR42J cells partly via a Myd88-dependent signaling pathway. *Arch. Biochem. Biophys.* **495** (1), 56–61 (2010).
25. Li, Y. Deoxyarbutin attenuates severe acute pancreatitis via the HtrA2/PGC-1α pathway. *Free Radic. Res.* ;**56**(9–10), 651–665 (2022).
26. Zhong, Z. et al. New mitochondrial DNA synthesis enables NLRP3 inflammasome activation. *Nature*. **560** (7717), 198–203 (2018).

27. Huang, Y. et al. Brown adipose TRX2 deficiency activates mtDNA-NLRP3 to impair thermogenesis and protect against diet-induced insulin resistance. *J. Clin. Investig.* **132** (9), e148852 (2022).
28. Jiang, M. et al. SIRT1 alleviates aldosterone-induced podocyte injury by suppressing mitochondrial dysfunction and NLRP3 inflammasome activation. *Kidney Dis. (Basel)*. **7** (4), 293–305 (2021).
29. Wan, W. et al. Grape seed proanthocyanidin extract moderated retinal pigment epithelium cellular senescence through NAMPT/SIRT1/NLRP3 pathway. *J. Inflamm. Res.* **14**, 3129–3143 (2021).

## Acknowledgements

This project received financial support from the Sichuan Provincial Department of Science and Technology (2022YFS0331) and Sichuan Provincial Heath Commission (21PJ083) and Sichuan Provincial People's Hospital HuanHua Talent Project (30420220153).

## Author contributions

SK.W. and W.L. wrote the main manuscript and J.Z. and F.W. devised and supported this work.

## Declarations

## Competing interests

The authors declare no competing interests.

## Statement

We are willing to pay the page charges if accepted for publication and the study are reported in accordance with ARRIVE guidelines.

## Additional information

**Supplementary Information** The online version contains supplementary material available at https://doi.org/10.1038/s41598-024-76825-9.

**Correspondence** and requests for materials should be addressed to F.W. or J.Z.

**Reprints and permissions information** is available at www.nature.com/reprints.

**Publisher's note** Springer Nature remains neutral with regard to jurisdictional claims in published maps and institutional affiliations.